



Postglacial landscape dynamics and fire regimes in west Central Patagonia, Chile (44°S, 72°W): Evidence from the Cisnes River Basin

Valentina Álvarez-Barra^{a,b}, Antonio Maldonado^{c,d,*}, María Eugenia de Porrás^e,
Amalia Nuevo-Delaunay^a, César Méndez^a

^a Centro de Investigación en Ecosistemas de la Patagonia (CIEP), José de Moraleda 16, 5950000, Coyhaique, Aysén, Chile

^b Estación Patagonia de Investigaciones Interdisciplinarias UC, Pontificia Universidad Católica de Chile, Avda. Vicuña Mackenna 4860, Macul, Santiago, Chile

^c Centro de Estudios Avanzados en Zonas Áridas (CEAZA), Raúl Bitran 1305, La Serena, Chile

^d Departamento de Biología Marina, Universidad Católica del Norte, Larrondo, 1281, Coquimbo, Chile

^e Instituto Argentino de Nivología, Glaciología y Ciencias Ambientales (IANIGLA), CCT Mendoza, CONICET, Mendoza, Argentina

ARTICLE INFO

Handling editor: Claudio Latorre

1. Introduction

West Central Patagonia (43°–47°S) is a key area for paleoenvironmental studies given its position within the area of influence of the Southern Westerly Winds (SWWs). Frontal precipitation systems migrating along storm tracks are intercepted by the Andes Cordillera, leading to contrasting climatic features on the western and eastern slopes of this mountain range. Thus, hyperhumid conditions prevail along the Pacific coast and windward slopes of the Andes, while dry conditions dominate leeward (Garreaud et al., 2013; Viale et al., 2019). Given that the precipitation gradient associated with the surface SWWs is responsible for the present-day vegetation gradient in Patagonia, numerous studies have focused on determining the position, latitudinal shifts, and strength of the changes of the SWWs at millennial to sub-centennial time scales, which have resulted in shifts in the position of ecotones, particularly the forest–steppe ecotone (Markgraf et al., 2007; McCulloch et al., 2000; Moreno, 2004; Whitlock et al., 2006).

In northern Patagonia (41°–43°S), Iglesias et al. (2014) described shifts in the position of the forest–steppe ecotone, indicating that periglacial areas were dominated by steppe communities ca >15,000 cal yr BP. Between 15,000 and 10,000 cal yr BP, the forest–steppe boundary advanced eastward and retreated in millennial-scale cycles from its actual position, shifting to an open *Nothofagus* forest during the Early Holocene and to a more closed forest toward the Late Holocene and associated with wetter conditions (Iglesias et al., 2014). In the Central Chilean Patagonia (44°S), the Lake Shaman record indicates the

easternmost position of the forest–steppe ecotone between 8000 and 3000 cal yr BP, suggesting the highest effective moisture with the establishment of strong seasonality between 5000 and 3000 cal yr BP (de Porrás et al., 2012).

Further south (45°S), the record from Mallín Pollux, located on the eastern side of the Andes, reflects that after glacial melting, a sparse scrub–steppe developed between 18,000 and 14,000 cal yr BP. A moderate increase in effective moisture triggered an expansion of steppe species by 14,000 cal yr BP followed by the establishment of a *Nothofagus*–steppe woodland at the beginning of the Holocene (11,000 cal yr BP; Markgraf et al., 2007). From 7500 cal yr BP onward the establishment of the present-day closed *Nothofagus* forest occurred, which was associated with the prevalence of the modern precipitation seasonality.

The record from Lago Augusta (47°S) spanning the last 16,000 cal yr BP in the Chacabuco River Valley indicates that herbs, shrubs, and evergreen rainforest taxa colonized areas that were previously inundated by proglacial lakes by ~15,600 cal yr BP under cold and wet conditions (Villa-Martínez et al., 2012). As with the abovementioned records, the transition toward the Holocene featured an expansion of the *Nothofagus* forest at the expense of steppe taxa, showing no forest taxa decline since 9800 cal yr BP until the last century, which is related to anthropogenic influence.

Records from the windward side of the Patagonian Andes also document the importance of the precipitation dynamics associated with the behaviors of the SWWs in determining past vegetation changes during the Last Glacial Maximum (LGM) and Termination 1, as

* Corresponding author. Centro de Estudios Avanzados en Zonas Áridas (CEAZA), Raúl Bitran 1305, La Serena, Chile.

E-mail addresses: antonio.maldonado@ceaza.cl, amaldona@userena.cl (A. Maldonado).

Glacial to recent times and comparing our findings with those records located further east. Notably in Patagonia, between 42° and 47°S, the Cisnes River Basin is the only east–west oriented valley that provides paleoecological records along the upper (east)-to-lower (west) river course, following the modern precipitation gradient.

2. Environmental setting

In West Central Patagonia (Fig. 1), geomorphological features indicate the ancient presence of glacier lobes, whose advances and retreats over millennial scales shaped the landscape's present topography (Cooper et al., 2021; Davies et al., 2020; García et al., 2019). The timing and extent of the ice lobes during the LGM and Termination 1 have been reconstructed based on geomorphological evidence and cosmogenic dating (Davies et al., 2018; García et al., 2019; Thorndycraft et al., 2019) and lacustrine sediment cores (de Porras et al., 2012; Vilanova et al., 2019) documenting the extensive dynamism of the landscape based on the changes in sedimentary features and pollen input at long-term scales.

The west–east oriented Cisnes River Basin is a clear example of a strong west–east precipitation gradient resulting from the rainshadow effect caused by the forced subsidence of surface air masses associated with the SWWs when they are intercepted by the Andes Cordillera. Thus, an annual precipitation of ~4000 mm is recorded at the western margin of the valley to <500 mm at its easternmost tip (Dirección Meteorológica de Chile, 2022). Precipitation variability at annual/interannual scales is controlled by the Southern Annular Mode (SAM). The positive phase of the SAM is associated with low (high) pressure anomalies over Antarctica (mid-latitudes), resulting in the strengthening and poleward contraction of the SWWs (warm and dry conditions over Patagonia; Abram et al., 2014; Moreno et al., 2018; Quade and Kaplan, 2017) while the negative phase results in an equatorward shift of the SWWs (cool conditions and increased precipitation over Patagonia; Marshall, 2003).

The sharp precipitation gradient, as well as the topography, are the primary drivers of the present-day vegetation distribution. Moreover, the Cisnes River Basin is characterized by altitudes <10 m a.s.l. at the river mouth (west) to > 960 m a.s.l. at its headwaters, the international Chile–Argentina border (east). In terms of vegetation, the vast areas of forests present at the mid- and high-latitudes of Patagonia are referred as Subantarctic forests, where communities located at mid-latitudes correspond to the North Patagonian rainforest, present mostly at the western margins of Patagonia (Luebert and Plissock, 2017). The areas located on the windward side of the Andes are dominated mostly by evergreen *Nothofagus* forest, while on the leeward side and further eastern areas, deciduous *Nothofagus* forest, the forest–steppe ecotone and the Patagonian steppe occur.

The west–east vegetation distribution along the Cisnes River Basin (Fig. 1b) includes the following.

- (1) The evergreen rainforest is characterized by the presence of evergreen *Nothofagus* species such as *N. betuloides*, *N. nitida* and *N. dombeyi*. The conifers *Podocarpus nubigenus* and *Pilgerodendron uviferum* (Cupressaceae) are also present, and when they dominate, the forest is called cold Patagonian rainforest (Luebert and Plissock, 2017). Other plants present within this forest are *Lomatia ferruginea*, *Amomyrtus luma*, *Aristotelia chilensis*, *Luma apiculata*, *Weinmannia trichosperma*, *Caldcluvia paniculata*, *Drimys winteri*, and *Embothrium coccineum*. The dominance of *W. trichosperma* associated with *Eucryphia cordifolia* defines the temperate rainforests. The annual average temperature in this area ranges between 8 and 10 °C, and the mean annual precipitation fluctuates between 3000 and 1000 mm (Hepp and Stolpe, 2014).
- (2) The temperate deciduous forest is mainly composed of deciduous *Nothofagus* species such as *N. pumilio* and *N. antarctica*. The presence of plants that also occur in the evergreen forest can be observed, resulting in *Nothofagus* forests mixed with *Dasyphyllum diacanthoides*, *Chiliotrichum diffusum*, *Berberis* sp., *Ribes*

magellanicum, *Lomatia hirsuta*, *Discaria* sp., *Colletia* sp., and *Chusquea* sp., among other species. The climatic gradient in this area fluctuates between 6 and 8 °C and 1000–2500 mean annual precipitation.

- (3) The forest–steppe boundary is composed primarily of shrubs such as *Gaultheria mucronata*, *Berberis microphylla*, *Discaria trinervis*, *Colletia spinosa*, *Schinus patagonicus*, and *Colliguaja integerrima*. Additionally, *Baccharis magellanica*, *Anemone multifida*, *Senecio patagonicus*, *Schoenus andinus*, *Oreobolus obtusangulus* characterized the herbaceous layer. *N. antarctica* is also present in the shrubland but adopts a tall shrub form. In this area, the temperature ranges from 6 to 8 °C, and the mean annual precipitation is 600–800 mm.
- (4) The Patagonian steppe is composed of species such as *Festuca gracillima*, *Stipa* sp., *Acaena leptacantha*, *Paspalum dilatatum*, *Azorella prolifera*, *Adesmia boronioides* and *Senecio neaei*. Here, the mean annual temperature is 4–6 °C, and the mean annual precipitation decreases to 400–600 mm (Hepp and Stolpe, 2014).

Past occupations of the Cisnes River Basin by hunter-gatherers have been studied with the aim of elucidating the timing and characteristics of the peopling process (Méndez and Reyes, 2008). While steppe environments have been seasonally and sporadically accessed since the Late Glacial/Holocene transition, archaeological investigations suggest that forests were initially visited during the Middle Holocene and recurrently incorporated into mobility after 3000 cal yr BP (Méndez et al., 2023). At this point, the western Cisnes River Basin was first occupied after 3000 cal yr BP, as indicated by the El Toro rock shelter record (Méndez and Reyes, 2008).

The role of indigenous populations in fire occurrence over the Central Chilean and Argentinean Patagonia has been largely studied (Iglesias and Whitlock, 2014; Maldonado et al., 2022; Méndez et al., 2016; Moreno et al., 2023; Nanavati et al., 2019), hypothesizing that hunter-gatherers contributed to enhancing fire activity at the regional scale since ~4000 cal yr BP, triggering changes in vegetation composition. However, some researchers argue that despite past indigenous populations contributing to modifying the timing of fires, they did not magnify the fire frequency in fire-prone environments (Méndez et al., 2016).

Anthropogenic disturbance has recently become more noticeably by the presence of introduced taxa such as *Pinus* sp. (monoculture), *Rumex acetosella*, *Plantago lanceolata*, *Taraxacum officinale*, *Dactylis glomerata*, *Holcus lanatus* and *Trifolium repens*, some of which are used for forage purposes. All these species colonized the area following the extensive burning of forests due to the creation of open areas by European and Chilean settlers during the beginning of the 20th century. Some research indicates that more than 3 million hectares of forest were burned (Bizama et al., 2011; Quintanilla, 2008), affecting the composition and structure of the forest. For instance, after large-scale disturbance, disturbed *Nothofagus nitida* and *Podocarpus nubigenus* forest were replaced by *N. nitida* and *Embothrium coccineum* associated with *Fuchsia magellanica* and *Aristotelia chilensis* (Luebert and Plissock, 2017). In contrast, disturbed swamp forests resulted in *mallines*, characterized by *Carex darwinii*, *Gunnera magellanica*, *Juncus procerus*, *Nertera granadensis*, and scattered *N. nitida* trees (Promis et al., 2013).

The Laguna Las Mellizas del Río Cisnes LLMRC (hereafter; 44°38'48.13" S; 72°19'42.58" W; 209 m a.s.l.), the present study site, is a small 6 m-deep lake located 1 km northeast of the Cisnes River, 27 km southeast of the Queulat Glacier and 27 km east of the Pacific coast of the Aysén region (Fig. 1b). The lake is surrounded by a ring of *Potamogeton*, while areas <1 m deep are colonized by *Juncus* sp., *Carex* sp., *Cyperus* and plants belonging to the Poaceae family. The immediate vicinity of the lake is characterized by the presence of arboreal elements such as *Nothofagus nitida*, *N. betuloides*, *N. antarctica*, *N. pumilio*, *Drimys winteri*, *Tepualia stipularis*, *Luma apiculata*, *Caldcluvia paniculata*, and *Weinmannia trichosperma*. The bamboo *Chusquea* and shrubs of *Gunnera*

are also present, as are *Mutisia*, *Hydrangea* and *Mitraria coccinea* among the climbing plants. The herbaceous plants include *Ranunculus*, *Digitalis* sp. (exotic), and Asteraceae species associated with Poaceae and *Blechnum penna-marina*. The vicinity of the lake is frequently used for cattle grazing.

3. Materials and methods

In 2015, a 470-cm-long sedimentary sequence was retrieved from the central part of the LLM_{RC} (water depth of 6 m at the coring point) using a modified Livingstone piston corer. The sedimentary sequence was visually characterized to describe the lithology, which was supported by X-ray analysis. Loss-on-ignition was analyzed contiguously at 1-cm intervals along the core to determine the organic and inorganic content, using 1-ml sample for the analysis (Heiri et al., 2001). The tephra layers present in the core were geochemically analyzed and related to their volcanoes and eruption sources by Weller et al. (2017).

The chronology of the sedimentary sequence from the LLM_{RC} was based on six bulk sediment samples carefully selected for radiocarbon dating. A previous age–depth model for this record was constructed by Weller et al. (2017) by applying the ShCal13 curve (Hogg et al., 2013). However, in this work, a new age–depth model was constructed based on adjusted depths after subtracting tephra layers with a thickness >1 cm, applying a smooth spline (0.1 smooth) with a 95% of confidence interval (1000 iterations) and considering 10-cm-thick sections to estimate the accumulation rate using the Bacon package (Blaauw and Christen, 2011) in the Rstudio interface (R Development Core Team, 2013) and calibrating the six radiocarbon dates with SHCal20 (Hogg et al., 2020).

Pollen samples of 1 cm³ were taken every 3 cm, avoiding tephra layers. Sample processing for pollen extraction was conducted following Faegri and Iversen (1989). A minimum of 500 pollen grains were counted to reduce the uncertainty of the frequency of less abundant pollen taxa (Birks and Birks, 1980), given the high pollen production of *Nothofagus* spp., the dominant tree in the forest. To calculate the pollen concentration (grains cm⁻³) and pollen accumulation rate (PAR, grains cm⁻² yr⁻¹), tablets of *Lycopodium clavatum* were added to each sample. The main pollen sum was based on the sum of trees, shrubs and herbs, while aquatic/paludal pollen and fern spores were calculated separately based on the main pollen sum described above. A pollen atlas (Heusser, 1971) and a pollen reference collection held at the Centro de Investigación en Ecosistemas de la Patagonia (CIEP) were used for pollen identification. Given the vegetation description and observations made during the field trip in the study area, we assumed that *Pilgerodendron uviferum* is contributing the most to the Cupressaceae pollen signal, as this cypress occurs in sites west of the LLM_{RC}, and modern studies in vegetation communities confirm the presence of *P. uviferum* in our study site (Luebert and Plissock, 2017).

To reconstruct the fire history, macroscopic charcoal particles were recovered contiguously along the core, avoiding the tephra layers. Subsamples of 1 cm³ were extracted from every centimeter sieved through a 125- μ m mesh and processed following the methodology outlined by Whitlock and Larsen (2001). Macro charcoal particles were observed and counted under a stereomicroscope. Macro charcoal counts were transformed to charcoal accumulation rates (CHARs; particles cm⁻² yr⁻¹) based on the above-described age model and analyzed using the software CharAnalysis (Higuera et al., 2009). The data were interpolated to the median sampling resolution (yr sample⁻¹) of the charcoal record (25 yr sample⁻¹). The charcoal background was estimated using a lowess smoother with a 500-year window. Peak events were detected using a locally defined threshold, and the noise distribution was determined by a Gaussian mixture model using the 99th percentile threshold. Fire frequency and fire return interval (FRI) were analyzed over a 1000-yr time window.

The pollen diagram and constrained cluster analysis (CONISS) were performed using Tilia 2.6.1 (Grimm, 2004). Pollen results were further

statistically analyzed, but zone M–1 was excluded from this analysis since the pollen percentages do not reflect local vegetation growing around the lake (see the Discussion section). To determine the most important direction of variation within the pollen dataset, a principal component analysis (PCA) was conducted using CANOCO 5.0 (Ter Braak and Smilauer, 2012) by transforming pollen percentage data to square roots to suppress the influence of dominant taxa. To evaluate the possible influence of fire on vegetation changes, we first performed a redundancy analysis (RDA) using CHAR, fire frequency, and fire magnitude as explanatory variables and selected pollen taxa percentages as response variables.

4. Results

4.1. Chronology and lithology

The six radiocarbon ages are in stratigraphic order and the age–depth model indicates an interpolated basal age of 13,909 cal yr BP and an average sample resolution of 113 years (Table 1)

Plotted against depth, the six dates follow a nearly linear curve (Fig. 2), and all the dates fall within the 95% confidence interval. Based on the age–depth model, a rapid sedimentation rate is observed between ~13,800 and ~12,100 cal yr BP (0.4 mm/yr). A decrease in the sedimentation rate is noticeable from ~11,100–~4500 cal yr BP (0.1 mm/yr), followed by an increase in the sedimentation rate from 4300 cal yr BP (0.7 mm/yr) onward. After 3100 cal yr BP, the sedimentation rate decreased to ~0.3 mm/yr.

The lithology of the sedimentary sequence of the LLM_{RC} is mainly composed by gyttja and sand with the presence of 18 volcanic ash horizons. The tephra deposits were identified using X-ray images while the source of the ashes was determined by lithostratigraphic data, petrography and bulk chemical analysis (Weller et al., 2017). A detailed description of the lithology is presented in Table 1S (Supplementary Material). Loss-on-ignition analysis revealed that from 470 to 393 cm, the percentage of organic matter was <1%, while from 392 to 368 cm this percentage varied between 5 and 20% (Fig. 3). Immediately after, the percentage of organic matter decreased to 1% (367–365), while the remainder of the core contained <40% organic matter, with some sections dominated by inorganic material (349–347 cm; 319–315 cm; 311 cm; 241–236 cm; 227–224 cm; 202 cm; 154 cm; and 105 cm). Most of these peaks of inorganic material correspond to the tephra layers along the sedimentary record of the LLM_{RC}, whose petrographic features were published by Weller et al. (2017). These were sourced by different eruption of volcanoes such as the Melimoyu, Mentolat, Hudson, Macá, and Cay (Fig. 3).

4.2. Pollen record

The pollen diagram shows that *Nothofagus dombeyi*-type, which includes *N. betuloides* (evergreen), *N. nitida* (evergreen), *N. antarctica* (deciduous) and *N. pumilio* (deciduous) dominates the record (Fig. 4). Based on the CONISS analysis, the pollen assemblages were subdivided into six major zones. In the lowest part of the record, Zone M–1 (443–368 cm, 13,909–12,494 cal yr BP), is dominated by pollen types such as *Nothofagus dombeyi*-type (<70% on average), *Podocarpus nubigenus* (<10%) and *Drimys* (<5%), although traces of Cupressaceae pollen (<3%; likely *Pilgerodendron uviferum*) are also present. Additionally, Ericaceae, Asteraceae and Poaceae, corresponding to shrub and herbaceous plants are also present during this period. Nevertheless, it is crucial to highlight that the PAR values of this section present an average of 1360 grains cm⁻² yr⁻¹ (Fig. 4), which is significantly lower than that of the rest of the record.

The following zone (M–2; 364–334 cm, 12,411–10,843 cal yr BP) showed a marked increase in the percentage of tree species such as *P. nubigenus* (<14%), and *Pilgerodendron* (<17%), while the average percentage of *Nothofagus* was approximately 26%. The appearance of

Table 1

AMS radiocarbon dates from the LLM_{RC} sediment core.

Lab ID	Depth (cm)	Adjusted depth (cm)	Material	Age (¹⁴ C yr BP)	±1 σ error	Median probability (cal yrs BP)
CO-surface	0–1	0	–	–	–	–65
D-AMS-30092	42	42.5	Bulk sediment	1120	25	1123
D-AMS-30093	109	105.5	Bulk sediment	2933	42	2977
D-AMS-30094	210	200.5	Bulk sediment	3929	48	4252
D-AMS-30095	293	272.5	Bulk sediment	5533	30	6282
D-AMS-30096	334	311.5	Bulk sediment	7626	37	8350
D-AMS-13302	366	360.5	Bulk sediment	10426	38	12075

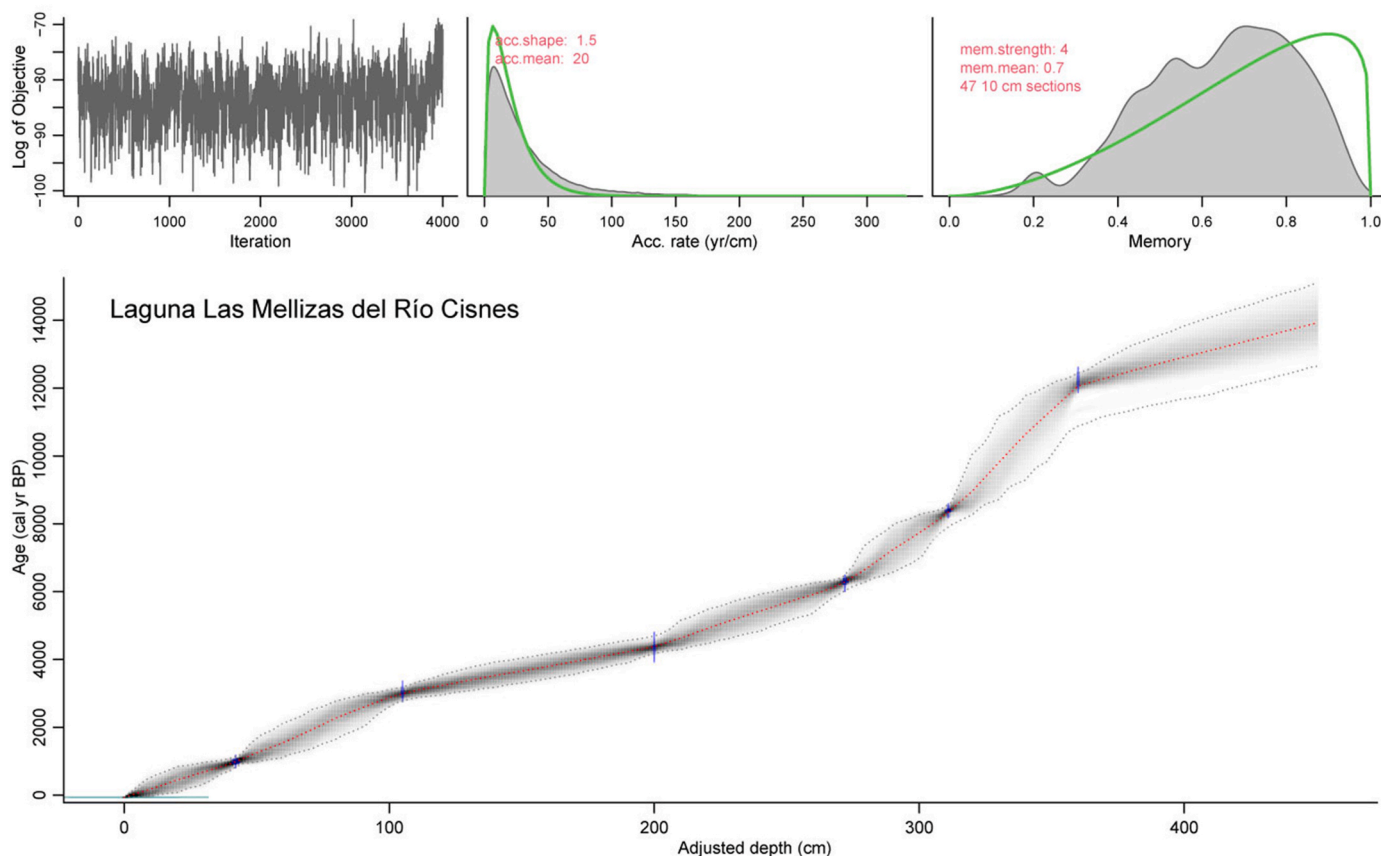


Fig. 2. Age–depth model of the LLM_{RC} record. The red line indicates the median probability age of the age model, while the gray shadow represents the 95% confidence interval. Blue lines represent the probability distribution of the calibrated radiocarbon ages.

Weinmannia trichosperma (<40%) during this period is a distinctive feature together with the presence of Myrtaceae family pollen grains (<8%; *Myrteola*, *Myrceugenia*, *Amomyrtus*, *Tepualia*). The mistletoe *Misodendrum* (<20%) is also characteristic of this zone. In turn, *Lycopodium magellanicum* and Polypodiaceae dominate (<5%) among the ferns (Fig. 4).

In comparison with those in the prior zone, the percentages of *N. dombeyi*-type (53%) and *P. nubigenus* (<19%), in zone M–3 (330–236 cm, 10,522–6437 cal yr BP) exhibit a constant increase, while those of *Pilgerodendron*, *W. trichosperma*, and *Misodendrum* decreased. Other elements such as *Lomatia/Gevuina* (<2%), *Raukaua laetevirens* (<2%), *Hydrangea* (<5%), *Maytenus* (<1%), and *Embothrium* (<1%), are also present. Regarding ferns, the percentage of *Polypodiaceae* decreases in comparison to the prior zone, while the percentage of *Lophosoria* slightly increases.

Zone M–4 (259–194 cm, 6250–4301 cal yr BP) features the highest percentage of *N. dombeyi*-type (64% on average) of the entire record (disregarding zone M–1 due to its low pollen concentration). During this period the percentages of *P. nubigenus* and *Pilgerodendron* decrease, as do

those of the vine *Hydrangea* and the exclusive *Nothofagus* spp. Parasite *Misodendrum*. Poaceae is slightly present during this period (1%). *Lophosoria* and Cyperaceae dominate among the ferns during this period (>4%).

In zone M–5 (190–24 cm, 4244–545 cal yr BP) there was a slight decrease in the percentage of *N. dombeyi*-type (55% on average) concomitant with an increase in the percentage of Poaceae (5%) and *Misodendrum* (7%) and negligible amounts of *Maytenus*, *Embothrium*, Ericaceae and Asteraceae. The percentage of Cyperaceae pollen remained stable during this period.

Finally, zone M–6 (20–0 cm, 441 cal yr BP to present) is characterized by a slight decrease in the percentages of *P. nubigenus*, *Hydrangea*, *Misodendrum*, and Poaceae. Within this zone, *Blechnum* reached its highest percentage (5%).

4.3. Fire record

Throughout the record, changes in fire activity are observed at millennial scales (Fig. 5). The signal-to-noise index (Kelly et al., 2011)

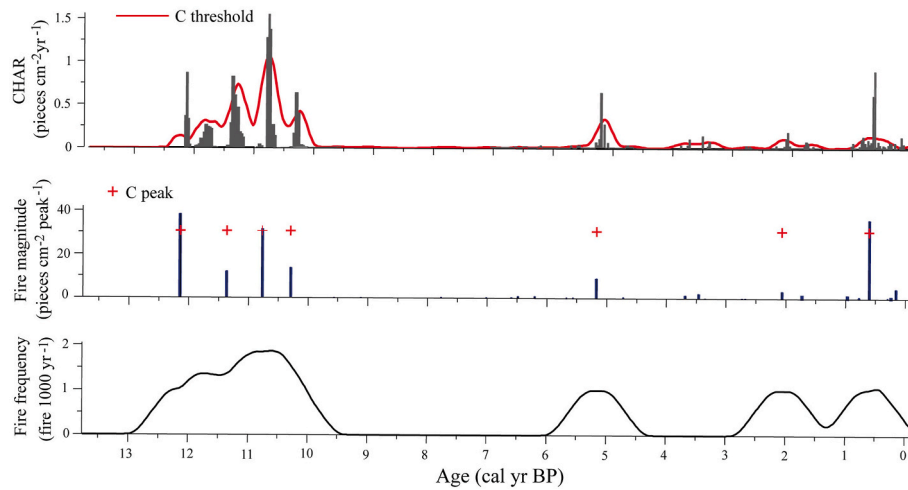


Fig. 5. Fire history for the LLM_{RC}.

presented values > 3 , indicating appropriate peak detection. The charcoal accumulation rates (CHARs) were normally < 2 pieces $\text{cm}^{-2} \text{yr}^{-1}$, and the CHAR background values were imperceptible throughout the record when the smoothing model was applied.

The first 1500 years of the record show no fire activity, but fire activity began at approximately 12,400 cal yr BP with a frequency of 1 fire per 1000 yr^{-1} . From 12,400 to 10,500 cal yr BP, the highest fire activity of the record was detected, as indicated by the occurrence of four fire episodes (charcoal peaks) with peak magnitudes at 12,135 cal yr BP (35 pieces $\text{cm}^{-2} \text{peak}^{-1}$), 11,300 cal yr BP (18 pieces $\text{cm}^{-2} \text{peak}^{-1}$), 10,600 cal yr BP (40 pieces $\text{cm}^{-2} \text{peak}^{-1}$) and approximately 10,100 cal yr BP (13 pieces $\text{cm}^{-2} \text{peak}^{-1}$), with fire frequencies reaching 1.2–2.3 fires 1000 yr^{-1} . Negligible fire activity was recorded at ~ 9500 – ~ 6200 cal yr BP, followed by an isolated peak at 5200 cal yr BP (8 pieces $\text{cm}^{-2} \text{peak}^{-1}$). Noticeable variability in fire frequency and fire magnitude is observed during the Late Holocene, with fire magnitudes under 8 pieces $\text{cm}^{-2} \text{peak}^{-1}$ but a major fire episode at ~ 500 cal yr BP.

4.4. Multivariate analysis

PCA revealed the main compositional trends in the pollen data, and a gradient of 1.2 SD suggested little variation within the data assemblages. The first axis explained 37% of the variance while the second axis 14%. The first axis contrasts *Weinmannia* and *Tepualia* with *N. dombeyi*. The first axis seems to be related to temperature influence: warm elements (*Weinmannia*, *Tepualia*) are ordered along positive values versus species adapted to cooler conditions (*N. dombeyi*) with negative values. The second axis contrasts Myrtaceae elements, *Podocarpus*, *Raukautia*, *Hydrangea*, and *Lomatia/Gevuina* with *Maytenus*, *Escallonia*, Asteraceae, and Ericaceae. This second component seems to arrange the species based on canopy configuration, with open vegetation characterized by shrubland elements (Ericaceae, Asteraceae, and *Maytenus*) ordered along positive values versus closed woodland dominated by species adapted to more humid and cold conditions (Myrtaceae, and *Podocarpus*) along negative values. Additionally, the second axis also indicates the direction of anthropogenic impact, represented by the introduced taxa *Rumex acetosella* and *Plantago lanceolata*, which are associated with forest clearance activities, and *Pinus* which is related to monospecific plantations.

Redundancy analysis revealed that the explanatory variables (fire analysis components) accounted for 12% of the total variation. Thus, fire frequency explained 10.9% of the variance, with a p value = 0.002, followed by CHAR (1.7%, $p = 0.086$) and fire magnitude (0.4%, $p = 1$). The RDA biplot (Fig. 7) shows that *Embothrium*, *Tepualia*, and *Weinmannia* are positively correlated with increased fire frequency. This may

imply that these taxa are partially favored by high fire activity, while periods with dominance of *N. dombeyi*-type and elements of the Myrtaceae family may be associated with low fire activity, as these taxa are negatively correlated with fire frequency. In turn, CHAR was positively correlated with *Maytenus*, *Misodendrum*, and *Pilgerodendron*; while fire magnitude was correlated with human indicator taxa (*Rumex*, *Plantago lanceolata* and *Pinus* sp.).

5. Discussion

5.1. Past vegetation, climate and disturbance

The pollen and the macroscopic charcoal record from the LLM_{RC} provide valuable insights into the changes in vegetation and environmental conditions in hyperhumid areas of West Central Patagonia since the Late Glacial/Holocene transition. In our record, the basal age of 13,900 cal yr BP is interpreted as a near-minimum age for the establishment of local ice-free conditions at the LLM_{RC}, inferred by the dominance of inorganic sediment (i.e., fine-sand particles) at the bottom section of the core (Fig. 3). Previous stratigraphic and geochronological evidence across the Cisnes River Basin suggests that glacier retreat occurred prior to 19,000 cal yr BP, with subsequent paleolake drainage and extensive landscape change (García et al., 2019). At 13,900 cal yr BP, we posit that the lake was not yet developed; instead, the inorganic matter present in the record was likely deposited in a small, relatively deep closed basin at the mountain foothills west of the LLM_{RC}. This environment might have provided suitable conditions for the establishment of Polypodiaceae ferns, as scarce pollen grains suggest. Furthermore, PAR values are low between 13,900 and 12,400 cal yr BP (Fig. 4) and the pollen signal from trees, shrubs and herbs captured in the LLM_{RC} record likely indicates either the scattered presence of those elements or long-distance transport from Subantarctic rainforest already developed to the west (Haberle and Bennett, 2004; Montade et al., 2013). Hence, we infer that the scarce pollen grains and low PAR found during this period imply an incipient process of landscape configuration (periglacial environment) and primary stages of postglacial area colonization in the lower Cisnes River Basin. Additionally, fire activity is absent during this interval, suggesting low biomass accumulation after glacier retreat as well as unsuitable climatic conditions for fire ignition and spread (cold and humid conditions).

Across the Cisnes River Basin, low magnitude and frequency of fires are observed in L. Shaman between 19,000 and 10,500 cal yr BP (de Porrás et al., 2012), while the record from Mallín El Embudo documents high magnitude and high-frequency fire episodes (7 fires 1000 yr^{-1}) between 13,000 and 10,500 cal yr BP (de Porrás et al., 2014). Both

records suggest ice-free but dry and cooler conditions at 19,000 and 13,000 cal yr BP (de Porras et al., 2012, 2014). Therefore, dissimilarities in fuel availability related to vegetation seem to explain the contrasting fire signals between sites along the Cisnes River Basin during the Late Glacial/Holocene transition (Fig. 8b). Conversely, the record from Mallín Pollux (Markgraf et al., 2007) shows moderate fire activity between 14,000 and 13,000 with increased fire episode frequency at 12,000 cal yr BP associated with warmer and drier conditions. This site shows that aridity continued after 14,000 cal yr BP, an opposite pattern than that observed in several records located between 41° and 46°S that actually document the establishment of the forest after 14,000 cal yr BP. This difference has been attributed mainly to the influence of glacial ice on the climate in sites east of the northern Patagonian icefield (Markgraf et al., 2003; 2007).

Organic lacustrine sedimentation occurs at ~12,300 cal yr BP characterized by gyttja (Fig. 3) coeval with increased PAR values, indicating a rapid process of plant colonization and the onset of the lake formation, with a sufficient water depth to support the development of *Potamogeton* and the establishment of the paludal Cyperaceae taxa (Fig. 4). Additionally, this transition is characterized by increased values of *N. dombeyi*-type and the mistletoe *Misodendrum*. Steady increases in *N. dombeyi* are also documented in Mallín El Embudo (44°S, 71°W; de Porras et al., 2014), L. Shaman (44°S, 71°W; de Porras et al., 2012), L. Augusta (47°S, 72°W; Villa Martínez et al., 2012) and L. Edita (47°S, 72°W; Henríquez et al., 2017) during the Late Glacial/Holocene transition, suggesting an increase in effective moisture in comparison to the prior period and the consequent development of scattered patches of *Nothofagus* trees. Additionally, *P. nubigenus* and *P. uviferum* show discrete but continuous percentage increases. Both are cold-tolerant hygrophilous trees, and their current occurrence is restricted to hyper-humid areas of Patagonia (Bannister et al., 2012; Luebert and Plischoff, 2017). Between the two species, *P. uviferum* dominates the first 400 years of zone M-2 with a peak of 17% at ~12,100 cal yr BP. The coeval presence of *P. nubigenus* and *P. uviferum* and *Nothofagus* recorded in the LLM_{RC} between 12,300 and 12,000 cal yr BP resembles the landscape reconstructed from L. Facil (44°S, 74°W) in the northern Chonos Archipelago (Haberle and Bennett, 2004). This assemblage is currently present in the southern part of the Chonos Archipelago (Luebert and Plischoff, 2017), characterized by humid and warmer conditions. Similarly, the MD07-3088 marine record from the Taitao Peninsula also documents this vegetation assemblage, interpreted as the expansion of the North Patagonian rainforest (Montade et al., 2013). Therefore, we conclude that humid and warm conditions allowed the onset of the expansion of *Nothofagus* trees in the Cisnes River Basin since 12,300 cal yr BP.

A noticeable shift in vegetation composition and climate is observed in zone M-2 with the rapid establishment of *W. trichosperma* since ~12,000 cal yr BP, associated with increased fire activity and contemporaneous with a decrease in the percentages of *N. dombeyi* and *P. uviferum* that we interpret as a decline in moisture. *W. trichosperma* is a characteristic tree of the temperate rainforest of Chile (Donoso, 2013; Lusk, 1999) and is also considered a paleoecological indicator of warmer conditions (Abarzúa et al., 2014; Haberle and Bennett, 2004; Moreno, 2020). It is also associated with disturbance events such as fires (Moreno et al., 2021). Its presence in the LLM_{RC} record likely accounts for an increase in summer temperatures as well as open conditions, as this tree is a shade-intolerant species (Donoso, 2013). Moreover, the dominance of *W. trichosperma* between 12,000 and 10,500 cal yr BP is concomitant with low but steady percentages of Myrtaceae elements (*Myrteola*, *Myrceugenia*, *Amomyrtus*, *Tepualia*) supporting the interpretation of an open landscape and warmer summers than present conditions at this latitude. These features are also observed in sites located north and west of the Andes which show high values of *W. trichosperma* (Abarzúa and Moreno, 2008; Jara and Moreno, 2014; Moreno, 2000). For example, the record from L. Negro (Fig. 8a—Moreno et al., 2021), located 77 km north of our record, shows peaks in the percentage of *W. trichosperma* (~56%)

between 11,900 and 10,700 cal yr BP coeval with decreasing percentages of *N. dombeyi*-type caused by disturbance and shifts in precipitation (Moreno et al., 2021). In this record, the authors conclude that the higher frequency and severity of the volcanic disturbance regime favored the abundance of shade-intolerant species, as the sites are located near the area of volcanic influence (Naranjo and Stern, 2004). In this respect, previous research on the LLM_{RC} core accounts for tephra layers from the Mentolat, Melimoyu, Hudson, Macá, and Cay volcanoes (Weller et al., 2017). The first volcanic tephra layer detected in the LLM_{RC} record is attributed to Macá/Cay or another minor eruptive center, after 12,000 cal yr BP with tephra layers <3 cm thick. Examining the probability of ash deposition influencing shifts in *W. trichosperma* percentages and fire, the LLM_{RC} record presents a tephra layer (2 cm thick; 9300 cal yr BP) deposited after the major increase in *W. trichosperma* (12,000–10,500 cal yr BP) that also followed high fire activity. Therefore, we posit that there is no direct correlation between tephra deposition and fire activity or between tephra deposition and *W. trichosperma* peak percentages.

Considering all these aspects, we conclude that the increase in *W. trichosperma* during the Early Holocene might be the result of a landscape configuration associated with persistent disturbance regimes, specifically fire. Nevertheless, even under favorable site conditions, *W. trichosperma* development and establishment succeed under certain climatic and forest structure conditions, i.e., temperate and open/semi open conditions, respectively. Overall, the increase in the percentage of *W. trichosperma* at the expense of *N. dombeyi*-type trees accounts for the replacement of the cold Patagonian rainforest by temperate forests associated with warmer conditions and enhanced rainfall seasonality (i.e., humid winters/dry summers), which in turn, favored fire ignition and spread, resulting in open patches for the establishment and development of *W. trichosperma*.

The Early Holocene (since 11,700 cal yr BP) in the LLM_{RC} record is characterized by the dominance of *W. trichosperma* and its later decrease at ~10,500 cal yr BP, followed by persistent increases in the percentages of *N. dombeyi* and *P. nubigenus*. Additionally, the highest fire activity observed across the record occurred during the Early Holocene, with three fire peaks at 11,300, 10,600, and 10,100 cal yr BP. The favorable climatic conditions might have resulted in the occurrence of fire, i.e., an increase in effective moisture that allowed vegetation development (associated mostly with increased *N. dombeyi*-type percentages) and continuity coupled with dry summers that enhanced the fire ignition probability and fire spread. Nevertheless, as the results obtained in the LLM_{RC} record indicate, fire was not meaningful west of the basin, as suggested by the low CHAR values (<2 pieces cm⁻² yr⁻¹). High fire activity during the Early Holocene was observed in several records in the eastern and western Andes between 41° and 47°S (Henríquez et al., 2017, 2021; Iglesias et al., 2011; Maldonado et al., 2022), although with differences in burned biomass (CHAR) likely explained by vegetation type and abundance.

By the time of decreasing percentages of *W. trichosperma*, the rise in *N. dombeyi* and *P. nubigenus* suggests the development of a closed *Nothofagus* forest, which is also reflected by the decrease in the percentage of *Misodendrum* (Fig. 4). This may imply a transition toward humid and cold conditions. At ~10,300 cal yr BP, *W. trichosperma* declines abruptly and *P. nubigenus* reaches its maximum percentage (21%) coeval with high Myrtaceae percentages, while fire activity is low (Fig. 5). Hence, we posit that increased effective moisture may have favored the development of a closed forest, therefore alleviating vertical fire continuity.

By comparing our results with those observed along the Cisnes River Basin, the Mallín El Embudo (48 km east of the LLM_{RC}) record shows increases in *N. dombeyi* concomitant with a decline in fire activity. The development of a closed *Nothofagus* forest since 9500 cal yr BP might have been associated with higher effective moisture than before and moderate dry summers (de Porras et al., 2014). For the steppe, the L. Shaman record (91 km northeast of the LLM_{RC}) reports high fire

frequency during the Early Holocene (5 fires 1000 yr⁻¹), with the highest peak at ~9600 cal yr BP (30 pieces cm⁻² yr⁻¹) and a later decrease in fire frequency and magnitude afterward (Fig. 8). This synchronous steady increase in the percentage of *N. dombeyi* and decline in that of Poaceae is likely associated with slight increases in effective moisture and the onset of forest–steppe ecotone development (de Porras et al., 2012).

The Middle Holocene epoch documented in the LLM_{RC} is characterized by a peak in the percentage of *N. dombeyi* (73%) at 7800 cal yr BP. The understory is dominated by the family Myrtaceae, accompanied by *Drimys*, *Embothrium coccineum* and *Raukautia laetevirens*. The liana *Hydrangea* is also present during this period. The intermittent percentages of *Potamogeton* suggest a variable water depth in the LLM_{RC}, which is supported by the fluctuations in the percentage of the paludal Cyperaceae. All these features are indicative of wet conditions and increased precipitation. The dominance of *N. dombeyi* during the Middle Holocene is also observed in the record from Mallín El Embudo (~80%) and L. Shaman (~60%) within the Cisnes River Basin. Southward, the record from L. Anónima (47°S, 72°W) shows the development of a closed *N. dombeyi* forest from 8200 cal yr BP, as a result of higher than present precipitation and reduced seasonality (de Porras et al., 2012, 2014; Maldonado et al., 2022). Taken together, the records mentioned above, including the LLM_{RC}, suggest that the establishment of the North Patagonian rainforest occurred during the Middle Holocene.

The timing of the establishment of the present-day North Patagonian rainforest in Patagonia during the Middle Holocene shows differences in some records from West Central Patagonia. However, most records agree that this period was characterized by increased precipitation. For instance, the present-day forest in the Chonos Archipelago was established at ~6000 cal yr BP (Haberle and Bennett, 2004). The pollen record of the MD07–3088 marine core near the Taitao Peninsula suggests that the modern conditions of the North Patagonian rainforest were reached after 5000 cal yr BP (Montade et al., 2013). These differences might reflect progressive responses of vegetation communities to variations in the position or expansion of the SWW belt since the Middle Holocene, influenced by the SAM which forces a north–south movement of the SWWs (Lee et al., 2019; Marshall, 2003). Positive SAM phases result in a poleward contraction of the SWWs, triggering warm conditions and decreased precipitation over Patagonia, while negative phases result in an equatorward shift in the SWWs associated with cool conditions and increased precipitation over Patagonia (Marshall, 2003). Therefore, we propose that the dominance of centennial-scale negative phases of SAM-like enhanced the cold and wet climate in Patagonia, allowing the progressive development and establishment of the *Nothofagus* forest across Patagonia.

The fire activity between 8000 and 4000 cal yr BP recorded in the LLM_{RC} is low, as shown in Fig. 5. This tendency is observed during the prior period since 10,500 cal yr BP, with unnoticeable fire activity and a discrete event at 5100 cal yr BP with a low CHAR value (<1 pieces cm⁻² yr⁻¹). Conversely, records located east of the LLM_{RC} show moderate fire activity during the Middle Holocene. For example, the Mallín El Embudo record shows CHAR values of <15 particles cm⁻² yr⁻¹ between ~8000 and ~4000 cal yr BP, peaking at ~4300 (78 particles cm⁻² yr⁻¹) and ~4000 (49 particles cm⁻² yr⁻¹). In turn, the L. Shaman record shows CHAR values < 20 particles cm⁻² yr⁻¹ during the Middle Holocene with major peaks at ~5800 cal yr BP (40 particles cm⁻² yr⁻¹) and ~4100 cal yr BP (46 particles cm⁻² yr⁻¹). All the records located along the Cisnes River Basin show similar-to-modern vegetation conditions during the Middle Holocene and wetter conditions than during the Early Holocene associated with intensified SWWs (de Porras et al., 2012, 2014). The pollen percentages in all these records also exhibit high values of *N. dombeyi*-type indicating fuel availability. These features suggest that the continuous fire activity in L. Shaman and Mallín El Embudo was likely influenced by dry summers but under permanent humid conditions that might have prevented severe fires. The low to absent fire activity documented in the LLM_{RC} for the Middle Holocene, despite the

presence of a dense *Nothofagus* forest, might be the result of the strong oceanic influence as the site is located 27 km from the Pacific coastline, resulting in strong frontal precipitation preventing fires in the humid forest.

Other paleoecological records from the Central Chilean Patagonia show cooler and wetter conditions by 5000 cal yr BP (Taitao Peninsula, 46°S; Montade et al., 2013); the establishment of a closed *Nothofagus* forest coeval with minimum fire activity and increased lake levels at 44°S between 7000 and 4000 cal yr BP (Mallín Fontanito; Nanavati et al., 2019); closed *Nothofagus* forest associated with high to low fire frequency from 8200 to 3800 cal yr BP (Lago Cochrane Valley, 47°S; Maldonado et al. (2022); and unaltered forest and low biomass burning from 6500 to 2000 cal yr BP in Mallín Casanova (47°S; Iglesias et al., 2018). Taking this together, the Middle Holocene in the Central Chilean Patagonia features wetter conditions than today, likely associated with the negative phase of SAM-like at the centennial scale (Lee et al., 2019). Those conditions triggered the development of a closed *Nothofagus* forest, preventing enhanced fire magnitude, although mild dry summers may have occurred as moderate fire frequency is reflected during this period in most of the records.

At approximately 4500 cal yr BP, the LLM_{RC} record documents the gradual increase in Poaceae coeval with shrubs and herbs (Ericaceae, Asteraceae) and a decrease in *N. dombeyi*-type percentages, although remaining the dominant taxa. Regarding vegetation composition, the understory is composed by *Fuchsia*, *Embothrium*, *Desfontainia*, Ericaceae, Rhamnaceae and Apiaceae, suggesting forest opening and a more diverse understory, likely promoted by a warm pulse that is inferred from the increase in the *W. trichosperma* percentage (Fig. 4). The pollen percentages of this tree show an increase between 2700 and 1600 cal yr BP, peaking at ~2300 cal yr BP (7%). As previously discussed, this species is associated with increased fire frequency, as the RDA indicates (Fig. 7). Hence, increased fire activity during the Late Holocene (ca. 4000 cal yr BP) clearly influenced the vegetation composition, facilitating *W. trichosperma* development and creating a forest opening, which in turn resulted in a more diverse understory (Fig. 4), and explaining the expansion of Poaceae during this period, specifically between 2700 and 640 cal yr BP.

By comparing with the records along the Cisnes River Basin, L. Shaman shows steady increases in Poaceae percentages during the abovementioned interval (de Porras et al., 2012), while Mallín El Embudo shows an opposite pattern (Fig. 8, de Porras et al., 2014). For L. Shaman, it is suggested that this shift in the percentage of Poaceae might reflect the retraction of the forest–steppe ecotone linked to decreased moisture at the easternmost portion of the Cisnes River basin. In turn, declining percentages of Poaceae documented in Mallín El Embudo reflect a process of expansion of the *Nothofagus* but still open forest compared with that observed in the record during the Early/Middle Holocene, likely associated with interannual or interdecadal fluctuations in moisture (de Porras et al., 2014). To sum up, the variations in *W. trichosperma* and Poaceae documented in the LLM_{RC} record are the result of the suitable conditions for fire ignition, i.e., fluctuations in moisture and warm conditions that favored fuel development and subsequent desiccation (Holz and Veblen, 2012).

The LLM_{RC} record features increased fire activity for the last 4000 cal yr BP (Fig. 5), coeval with changes in forest composition, i.e., forest opening and increased percentage of Poaceae (Fig. 4). The RDA shows that fire magnitude is positively correlated with Poaceae while *N. dombeyi*-type is oppositely ordered with fire frequency (Fig. 7). High fire activity during the Late Holocene is also observed in several records from Central Chilean Patagonia previously discussed (L. Facil, L. Oprasa, Mallín Fontanito, Mallín Casanova, L. Anónima). Possible drivers of this increased fire activity across Patagonia are examined in various studies, indicating the primary influence of positive phases of SAM as a driver of natural fire occurrence in forested regions where fire activity depends on fuel desiccation (Holz et al., 2017; Moreno et al., 2010b). Indeed, Moreno et al. (2023) concluded that hydroclimatic variations are a

primary driver of fire activity along the western Andes between 40°S and 44°S in the Chilean Patagonia. Although some of the records along the Cisnes River Basin are located at the eastern slopes of the Andes (L. Shaman and Mallín El Embudo), they are certainly influenced by changes in the SWWs during the Late Holocene via modulation of the precipitation seasonality and therefore of fire intensity and occurrence. The fire magnitude detected in the LLM_{RC} record during the Late Holocene is overall low (<2 pieces cm⁻² yr⁻¹) with a noticeable event at 600 cal yr BP (36 pieces cm⁻² yr⁻¹). However, the fire magnitude is substantively greater in the L. Shaman record with values < 14,800 pieces cm⁻² yr⁻¹ (peaks at ~4200, 3200, 2800, 2300, 900, 500 and 200 cal yr BP) and Mallín El Embudo with values < 3400 pieces cm⁻² yr⁻¹ (peaks at ~4300, 4200, 4000, 3900, 3000, 1500, and 200 cal yr BP). These dissimilarities may result from a compound climate–fire–vegetation relationship during the Late Holocene across the Cisnes River Valley, occurring at the different vegetation units along the west–east vegetation and climatic gradient. Nevertheless, the asynchronies in fire activity could be partially related to human activity (Méndez and Reyes, 2008; Méndez et al., 2011).

After 4000 cal yr BP, the LLM_{RC} pollen diagram shows a persistent decline in the percentage of Myrtaceae family elements (*Myrteola*, *Myrceugenia*, *Amomyrtus*, *Tepualia*). Currently, these taxa occur in flooded terrains in the study area, most of them disturbed by human activities such as burning and intensive grazing (Promis et al., 2013). The decline in the Myrtaceae element percentages during the Late Holocene may be due to changes in ecological niches triggered by a forest opening process, resulting in increased shrub and herb diversity (Figs. 4 and 6) at the expense of Myrtaceae elements. Previous studies indicate that most of the Myrtaceae genera identified in the LLM_{RC} occur within humid, dense and shady forests (Donoso, 2013; Luebert and Plischoff, 2017; Promis et al., 2013; Retamales, 2021). As illustrated in the PCA plot (Fig. 6), the presence of Myrtaceae is linked to forested landscapes. Hence, we postulate that temperate conditions coupled with precipitation seasonality favor the colonization and expansion of shrubs and herbs in open areas, limiting the development and establishment of Myrtaceae.

The last 500 years of vegetation history documented in the LLM_{RC} are characterized by a slight increase in *N. dombeyi*-type (>60%) and decreased abundance of *P. nubigenus*, Poaceae and traces of Myrtaceae coeval with diverse shrubs and herbs (Fig. 4). These features suggest the presence of a closed forest, similar to the one observed at present.

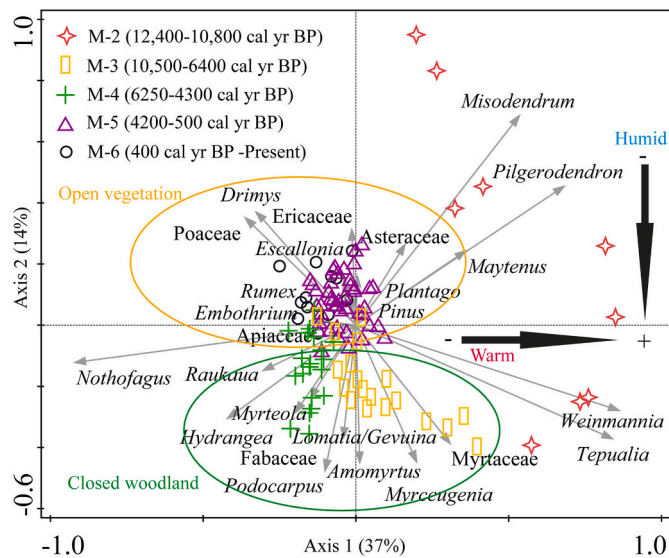


Fig. 6. PCA scatterplots of samples and selected taxa from the LLM_{RC}. The ellipses group open vegetation indicator taxa (upper yellow ellipse) and closed woodland indicator taxa (lower green ellipse).

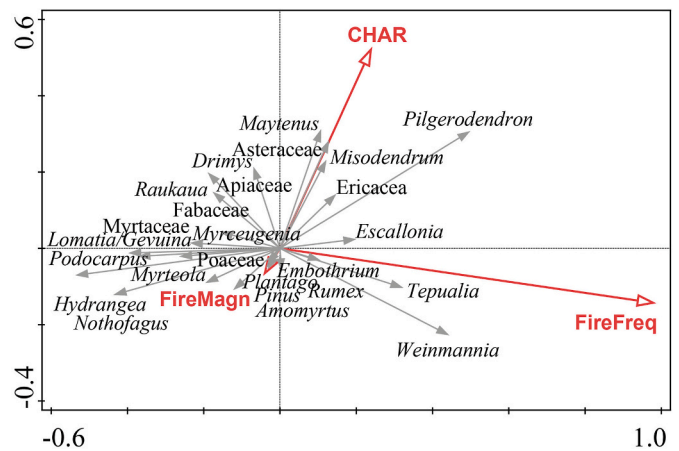


Fig. 7. RDA biplot of fire variables and selected pollen taxa from the LLM_{RC}.

However, the Chilean government, as an initiative for the colonization of remote areas, promoted clearance practices for human settlement, agriculture and livestock development and to create routes for communication. Starting in the 20th century, this process involved the burning of millions of hectares of native forest in the Aysén region (Bizama et al., 2011; Martinic, 2005; Otero, 2006; Quintanilla, 2008), resulting in the loss and fragmentation of the original forest. The first introduced taxon detected in the LLM_{RC} record is *Rumex acetosella* at 1900 AD, followed by *Plantago lanceolata* and *Pinus* (1960 AD). Despite these findings, we presume that given the topography and limited access to the study site, recent human activities did not result in significant changes in vegetation composition, contrary to the pattern observed in other records located further east (L. Venus, Szeicz et al., 1998; Mallín El Embudo, de Porras et al., 2014; Mallín Pollux, Markgraf et al., 2007) where human settlement imprint was more intense. Moreover, the vegetation unit characteristics of the abovementioned sites are also a factor to be considered, given their proximity to the forest–steppe ecotone, where surface fires are common and frequent, triggering vegetation changes.

The anthropogenic origin of fires is of paramount importance in Patagonia, as comparative studies have suggested that past communities, either purposefully or accidentally, may have influenced fire regimes at some points in time (Holz et al., 2016). A marked rise in the number of radiocarbon-dated archaeological sites as well as increased artifact deposition suggest enhanced human activity during the Late Holocene which has been interpreted as a meaningful contribution to the heightened occurrence of fire activity both west (Chonos Archipelago) and east (Cisnes river basin) of the LLM_{RC} site (Méndez et al., 2016; Moreno et al., 2023). El Toro Rock Shelter, located only 16 km from the LLM_{RC}, is a unique site in the forest of the region, with occupations dating to 2700 cal yr BP (Méndez and Reyes, 2008). Its occupation, however, does not coincide with any fire peak in the LLM_{RC} record, suggesting no influence of human activity as a potential trigger for fires in this record.

5.2. Regional discussion

As previously discussed, the palaeoecological information gathered in West Central Patagonia shows contrasting signals regarding past vegetation, climate, and disturbance history, although some records capture similar trends. For example, the records from L. Oprasa and L. Facil, located in the Chonos Archipelago (Haberle and Bennett, 2004), and the record from L. Negro (Moreno et al., 2021) show similarities with the LLM_{RC} record at a regional scale. For instance, the timeframe of the increase in *P. uviferum* in these sites occurs between 12,700 and 10,900 cal yr BP but with a ~200 year delay in the LLM_{RC}. Similarly, the period of increase in *W. trichosperma* occurs mostly during the Early

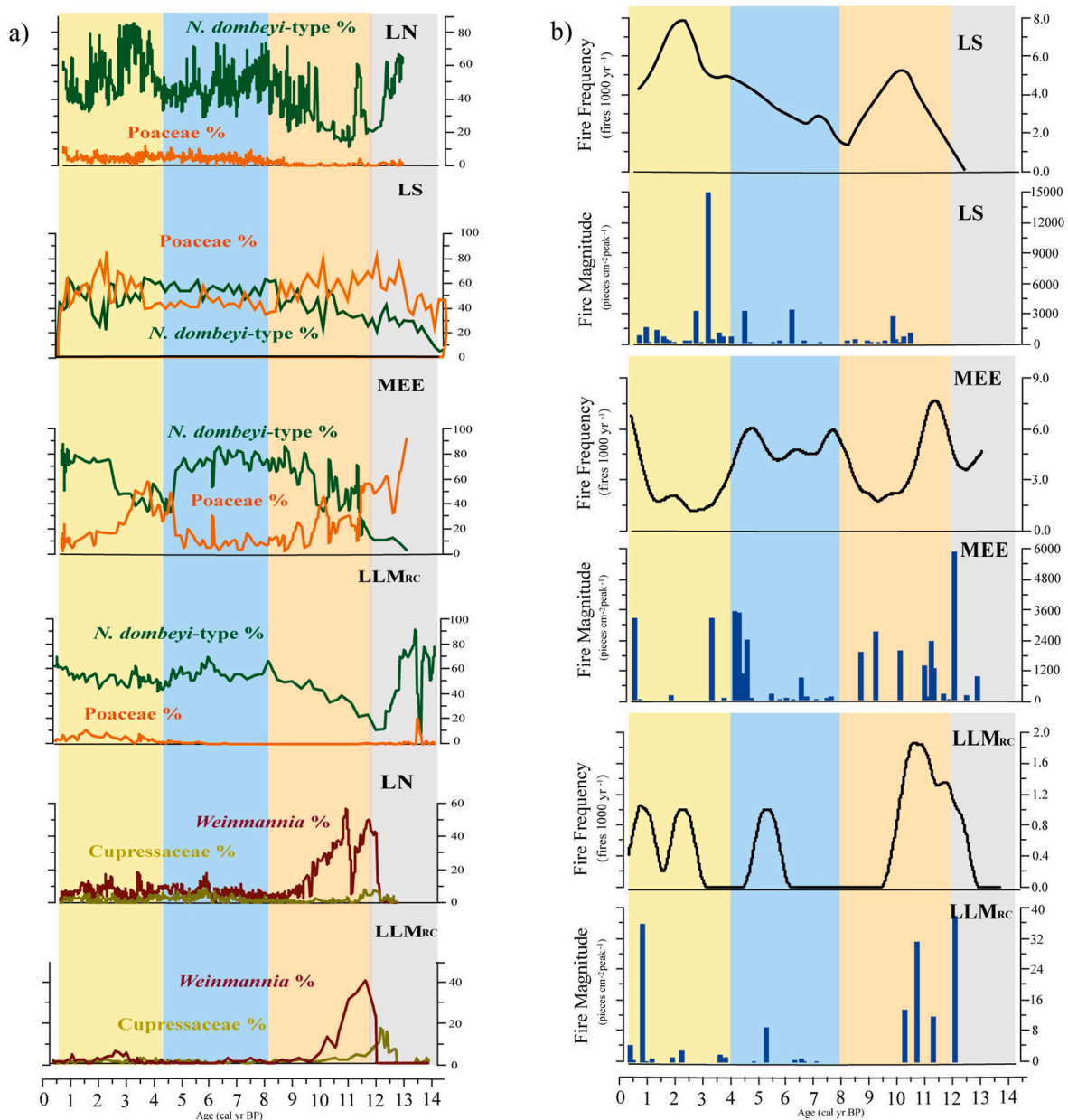


Fig. 8. (a) Selected taxa percentage curves from L. Negro (LN), L. Shaman (LS), Mallín El Embudo (MEE) and Laguna Las Mellizas del Río Cisnes (LLM_{RC}); (b) Fire history from the LS, MEE and LLM_{RC}. The Y-axis indicates the individual values of each curve. Different colors define millennial time periods discussed in the text (from left to right: Late Holocene, Middle Holocene, Early Holocene, Holocene/Late Glacial transition, Late Glacial).

Holocene, although we observed that the LLM_{RC} record documents the increase in this species 2000 years before (Late Glacial/Holocene transition) the L. Oprasa and L. Facil records. Nevertheless, the LLM_{RC} record documents maximum percentages of *W. trichosperma* almost at the same time as the L. Negro record, located perpendicularly north from the LLM_{RC} (Fig. 1). As discussed previously, fire-related disturbance is a paramount driver in modeling vegetation composition in Patagonia, associated with warm and humid conditions for forest development and establishment, i.e., fuel availability, followed by a period of enhanced precipitation seasonality coupled with increases in summer temperatures that allow fire ignition and spread. The observed differences in vegetation dynamics in these sites can likely be interpreted as a step wise response to climatic aspects at a local scale influenced by disturbance events (volcanism and fire).

Another important aspect observed in the records from West Central Patagonia is the persistence of the North Patagonian Forest, dominated

by *Nothofagus* species. Some studies show unaltered closed-*Nothofagus* forest from 9400 cal yr BP (L. Mellizas-Coyhaique, Villa-Martínez and Moreno, 2021) and from 10,000 cal yr BP (L. Churrasco, Moreno et al., 2019), despite the occurrence of disturbance (volcanism and fire) and climate change. Both sites are located at 45°S within the deciduous *Nothofagus* forest, hence, they are not sensitive to the Holocene changes of relatively minor magnitude. Indeed, modern pollen rain around these lakes presents values of *Nothofagus* values that fluctuate between 80 and 90% (Álvarez-Barra unpublished data), supporting the idea that *Nothofagus* pollen is overrepresented by local or long distance production and dispersion.

Asynchronies in vegetation responses and/or the absence of response to climatic forces are interpreted as differences in terms of the sensitivity of the records to the influence of, for example, the latitudinal expansion or retractions of the Southern Westerly Winds (SWWs, Maldonado et al., 2022; Villa-Martínez et al., 2012). The SWWs are a component of the

global atmospheric system that controls the climate of regions between 30° and 60°S (Fletcher and Moreno, 2011; Garreaud, 2009; Garreaud et al., 2013). Changes in its latitudinal position as well as strength dictate the moisture regimes in the middle-to higher-latitude in southern South America (Moreno et al., 2018). Given its importance, most analyses of the palaeoecological records located within the area of influence of the SWWs seek to understand past patterns of SWW behavior (Fletcher and Moreno, 2011; Moreno et al., 2010a; Villa-Martínez and Moreno, 2007). It has been suggested that the dominance of Magellanic deciduous forest and North Patagonian rainforest might be interpreted as evidence for relative wetter conditions and increased influence of the SWWs (Moreno et al., 2010a). Conversely, periods with decreases in *Nothofagus* and increases in Poaceae (interpreted as a forest opening) are related to weaker SWWs, i.e., drier conditions (Moreno et al., 2010a). Additionally, the location of the forest–steppe ecotone is dependent on moisture balance, which is also dictated by the amount of precipitation derived from the SWWs eastward over the Andes (de Porras et al., 2012; Páruelo et al., 1998). Most of the records in Patagonia show dissimilarities throughout the latitudinal range of SWW influence, and this might be related to (i) the location of the sites within the area of displacement of the SWWs (latitudinal shifts); (ii) specific topographic condition where the sites are located (e.g. plain or mountainous sites, height, etc.); (iii) microclimatic conditions present across Patagonia; (iv) west–east orientation of the sites and (v) proximity to areas of strong geomorphological changes (foothills, volcanoes, periglacial areas, among others).

In addition to the role of the SWWs in controlling overall vegetation changes in Patagonia, the Southern Annular Mode (SAM) has also been described as a factor that explains centennial-scale anomalies in precipitation and temperature in southern latitudes (Davies et al., 2020; de Porras et al., 2012; Holz and Veblen, 2012; Moreno et al., 2010a, 2014). A modern pollen–climate calibration, indicates that summer precipitation and winter temperature represent the main climate parameters controlling vegetation distribution in western Patagonia (Montade et al., 2019). Here, negative SAM modes are related to cold and wet conditions, while positive SAM modes are associated with warm and dry conditions (Davies et al., 2020; Quade and Kaplan, 2017). Changes at centennial timescales of the SAM have been analyzed in southern Patagonia, indicating that during positive SAM phases fire activity increases, triggering forest fragmentation and lake level decreases, while negative SAM phases are linked to muted fire activity, increases in lake levels and the establishment of closed-canopy forest (Moreno et al., 2014). The influence of the SAM on variations in climate and vegetation over Patagonia at decadal/centennial scales has also been reported in several records (de Porras et al., 2012; Maldonado et al., 2022; Moreno et al., 2021). Overall, we posit that the changes observed in fire activity and vegetation documented in the LLM_{RC} record are certainly influenced at a regional/millennial-scale by changes in the SWWs and at a local/centennial-scale by SAM-like phases.

6. Conclusions

The lacustrine sediment core from the LLM_{RC} documents noticeable changes in plant communities as well as fire regimes since the Late Glacial/Holocene transition in the westernmost part of the Cisnes river basin, in the Aysén region. Ongoing plant colonization is inferred since 13,900 cal yr BP until 12,400 cal yr BP as reflected by the low PAR values. The fire record does not show fire occurrence during this period as a potential result of the low available biomass coupled with a lack of vegetation continuity for fire to spread and unfavorable climatic conditions for fire ignition. Drastic shifts in environmental conditions occurred after 12,300 cal yr BP according to the onset of organic gyttja deposition along with an increase in *Nothofagus* percentages coeval with increased percentages of the mistletoe *Misodendrum*, suggesting an increase in effective moisture, which might have facilitated the expansion of the North Patagonian rainforest at ~44°S.

A rise in temperature is inferred by the substantial increase in the percentage of *W. trichosperma*, a shade-intolerant pioneer species characteristic of the temperate forest between 12,000 and 10,500 cal yr BP. This feature marks the Late Glacial/Early Holocene transition associated with enhanced fire activity, a common pattern observed along the Cisnes river valley. Multivariate analysis revealed a significant correlation between fire frequency and *W. trichosperma* percentages. This agrees with the fact that this tree is favored by fire disturbance, an ecological pattern that has been attested in several studies, suggesting a regional response of this species between 11,100 and 9300 cal yr BP associated with increased summer temperature.

The North Patagonian rainforest expanded and established around the LLM_{RC} at the beginning of the Middle Holocene (8000 cal yr BP), replacing the temperate rainforest. In conjunction with the dominance and high diversity of the Myrtaceae family elements, the substantial dominance of the *Nothofagus* forest is associated with the decrease in fire frequency and low CHAR values between ~8000 and ~4000 cal yr BP suggesting humid conditions throughout the Middle Holocene, a pattern detected also in nearby records, implying overall higher than present precipitation and reduced seasonality in West Central Patagonia.

The last 4500 cal yr BP in our record shows a gradual increase in Poaceae percentages together with increases in Ericaceae and Asteraceae, at the expense of *N. dombeyi*-type. An increased diversity of shrubs and herbs during this period is interpreted as forest opening, likely triggered by a warm pulse, associated with the increase in *W. trichosperma*, linked to the SAM short scale variability. Fire activity during this period shows an increase in frequency and magnitude, likely associated with positive SAM activity. The anthropogenic influence by indigenous populations settled in the Aysén region on the fire dynamics has been hypothesized in earlier studies. Although human occupations close to the LLM_{RC} are documented at ~2700 cal yr BP (El Toro rock shelter), our results suggest no influence of human activity as potential triggers for fires during the last 4000 years. Overall, the record from the LLM_{RC} offers a singular history of past vegetation and fire regimes at the westernmost part of the Cisnes river basin, within the dense evergreen rainforest of West Central Patagonia, pointing out the primary influence of SAM-like activity on the SWs, resulting in changing vegetation communities, as well as variations in fire activity over time.

Declaration of competing interest

The authors declare that they have no known competing financial interests that could have appeared to influence the work reported in this paper.

Data availability

Aspects of the record are available upon request to the corresponding author.

Acknowledgment

We thank Constanza Maldonado for helping during fieldwork and Rodrigo Álvarez for allowing access to L. Las Mellizas del Río Cisnes. We thank P.I. Moreno for facilitating the data from L. Negro and Hospital Público San Pablo for allowing the X-ray analysis of the cores. We acknowledge funding from ANID-FONDECYT 1210042; ANID-FONDECYT 3220115; ANID Regional R20F0002; and National Geographic Society #HJ-150R-17 grants.

Appendix A. Supplementary data

Supplementary data to this article can be found online at <https://doi.org/10.1016/j.quascirev.2024.108655>.

References

- Abarzúa, A.M., Moreno, P.I., 2008. Changing fire regimes in the temperate rainforest region of southern Chile over the last 16,000 yr. *Quat. Res.* 69, 62–71. <https://doi.org/10.1016/j.yqres.2007.09.004>.
- Abarzúa, A.M., Pichincura, A.G., Jarpa, L., Martel-Cea, A., Sterken, M., Vega, R., Pino, M., 2014. Environmental responses to climatic and cultural changes over the last 26000 years in Purén-Lumaco valley (38°S). In: Dillehay, Tom D. (Ed.), *The Telescopy Polity*. Springer, New York. https://doi.org/10.1007/978-3-319-03128-6_6.
- Abram, N.J., Mulvaney, R., Vimeux, F., Phipps, S.J., Turner, J., England, M.H., 2014. Evolution of the Southern Annular mode during the past millennium. *Nat. Clim. Chang.* 4, 564–569. <https://doi.org/10.1038/nclimate2235>.
- Bannister, J.A., Donoso, P.J., Bauhus, J., 2012. Persistence of the slow growing conifer *Pilgerodendron uviferum* in old-growth and fire-disturbed southern bog forests. *Ecosystems* 15, 1158–1172. <https://doi.org/10.1007/s10021-012-9574-7>.
- Birks, H.J.B., Birks, H.H., 1980. *Quaternary Palaeoecology*. Edward Arnold, London.
- Bizama, G., Torrejón, F., Aguayo, M., Muñoz, M.D., Echeverría, C., Urrutia, R., 2011. Pérdida y fragmentación del bosque nativo en la cuenca del río Aysén (Patagonia-Chile) durante el siglo XX. *Rev. Geogr. Norte Gd.* 49, 125–138. <https://doi.org/10.4067/S0718-34022011000200008>.
- Blaauw, M., Christen, J.A., 2011. Flexible paleoclimate age-depth models using an autoregressive gamma process. *Bayesian Anal.* 6, 457–474. <https://doi.org/10.1214/11-BA618>.
- Cooper, E.-L., Thorndyraft, V.R., Davies, B.J., Palmer, A.P., García, J.-L., 2021. Glacial geomorphology of the former Patagonian ice sheet (44–46°S). *J. Maps* 17 (2), 661–681. <https://doi.org/10.1080/17445647.2021.1986158>.
- Davies, B.J., Thorndyraft, V.R., Fabel, D., Martin, J.R.V., 2018. Asynchronous glacier dynamics during the antarctic cold reversal in central Patagonia. *Quat. Sci. Rev.* 200, 287–312. <https://doi.org/10.1016/j.quascirev.2018.09.025>.
- Davies, B.J., Darvill, C.M., Lovell, H., Bendle, J.M., Dowdeswell, J.A., Fabel, D., García, J.-L., Geiger, A., Gasser, N.F., Gheorghiu, D.M., Harrison, S., Hein, A.S., Kaplan, M.R., Martin, J.R.V., Mendelova, M., Palmer, A., Pelto, M., Rodés, A., Sagredo, E.A., Smedley, R.K., Smellie, J.L., Thorndyraft, V.R., 2020. The evolution of the Patagonian Ice Sheet from 35 ka to the present day (PATICE). *Earth Sci. Rev.* 204, 103152. <https://doi.org/10.1016/j.earscirev.2020.103152>.
- de Porras, M.E., Maldonado, A., Abarzúa, A.M., Cárdenas, M.L., Francois, J.P., Martel-Cea, A., Stern, C.R., Méndez, C., Reyes, O., 2012. Postglacial vegetation, fire and climate dynamics at central Chilean Patagonia (Lake Shaman, 44°S). *Quat. Sci. Rev.* 50, 71–85. <https://doi.org/10.1016/j.quascirev.2012.06.015>.
- de Porras, M.E., Maldonado, A., Quintana, F.A., Martel-Cea, A., Reyes, O., Méndez, C., 2014. Environmental and climatic changes in central Chilean Patagonia since the late glacial (Mallín el Embudo, 44°S). *Clim. Past* 10, 1063–1078. <https://doi.org/10.5194/cp-10-1063-2014>.
- Dirección Meteorológica de Chile, 2022. Informe de temperaturas y precipitaciones. <http://climatologia.meteochile.gob.cl/application/diario/boletinClimatologicoDiario/actual>. (Accessed 20 June 2022).
- Donoso, C., 2013. *Las especies arbóreas de los bosques templados de Chile y Argentina*. Autoecología, Valdivia, Chile.
- Fægri, K., Iversen, J., 1989. *Textbook of Pollen Analysis*. John Wiley & Sons Ltd, Londres.
- Fletcher, M.S., Moreno, P.I., 2011. Zonally symmetric changes in the strength and position of the Southern Westerlies drove atmospheric CO₂ variations over the past 14 k.y. *Geology* 39 (5), 419–422. <https://doi.org/10.1130/G31807.1>.
- García, J.-L., Maldonado, A., de Porras, M.E., Nuevo Delaunay, A., Reyes, O., Ebensperger, C.A., Binnie, S.A., Lithgens, C., Méndez, C., 2019. Early deglaciation and paleolake history of río Cisnes glacier, Patagonian ice sheet (44°S). *Quat. Res.* 91 (1), 194–217. <https://doi.org/10.1017/qua.2018.93>.
- Garreaud, R., 2009. The Andes climate and weather. *Adv. Geosci.* 22, 3–11. <https://doi.org/10.5194/adgeo-22-3-2009>.
- Garreaud, R., López, P., Minvielle, M., Rojas, M., 2013. Large-scale control on the Patagonian climate. *J. Clim.* 26, 215–230. <https://doi.org/10.1175/JCLI-D-12-00001.1>.
- González, M.E., Veblen, T.T., Sibold, J.S., 2010. Influence of fire severity on stand development of *Araucaria araucana*-*Nothofagus pumilio* stands in the Andean cordillera of south-central Chile. *Austral Ecol.* 35, 597–615. <https://doi.org/10.1111/j.1442-9993.2009.02064.x>.
- Grimm, E., 2004. *Tilia and TiliatView 2.0* Software Illinois State Museum. Research and Collection Center, Springfield, USA. <https://www.tiliait.com/>.
- Haberle, S.G., Bennett, K.D., 2004. Postglacial formation and dynamics of North Patagonian rainforest in the Chonos Archipelago, southern Chile. *Quat. Sci. Rev.* 23, 2433–2452. <https://doi.org/10.1016/j.quascirev.2004.03.001>.
- Heiri, O., Lotter, A., Lemcke, G., 2001. Loss on ignition as a method for estimating organic and carbonate content in sediments: reproducibility and comparability of results. *J. Paleolimnol.* 25, 101–110. <https://doi.org/10.1023/A:1008119611481>.
- Henríquez, W.I., Villa-Martínez, R., Vilanova, I., De Pol-Holz, R., Moreno, P.I., 2017. The last glacial termination on the eastern flank of the central Patagonian Andes (47°S). *Clim. Past* 13, 879–895. <https://doi.org/10.5194/cp-13-879-2017>.
- Henríquez, C.A., Moreno, P.I., Lambert, F., Alloway, B.V., 2021. The role of climate and disturbance regimes upon temperate rainforests during the Holocene: a stratigraphic perspective from Lago Fonk (~40°S), northwestern Patagonia. *Quat. Sci. Rev.* 258, 106890. <https://doi.org/10.1016/j.quascirev.2021.106890>.
- Hepp, K.C., Stolpe, B.N., 2014. Caracterización y propiedades de los suelos de la Patagonia Occidental (Aysén) [en línea]. Coyhaique, Chile: Boletín INIA - Instituto de Investigaciones Agropecuarias no. 298. Disponible en: <https://hdl.handle.net/20.500.14001/7793> (Consultado: 31 agosto 2023).
- Heusser, C.J., 1971. *Pollen and Spores of Chile*. University of Arizona Press, Arizona.
- Heusser, C.J., Heusser, L.E., Lowell, T.V., 1999. Paleoeology of the Southern Chilean Lake District-Isla Grande de Chiloé during middle-late Llanquihue Glaciation and Deglaciation. *Geogr. Ann.: Phys. Geogr.* 81, 231–284. <https://doi.org/10.1111/1468-0459.00058>.
- Heusser, L.E., Heusser, C.J., Mix, A., McManus, J., 2006. Chilean and Southeast Pacific paleoclimate variations during the last glacial cycle: directly correlated pollen and δ18O records from ODP Site 1234. *Quat. Sci. Rev.* 25, 3404–3415. <https://doi.org/10.1016/j.quascirev.2006.03.011>.
- Higuera, P.E., Brubaker, L.B., Anderson, P.M., Hu, F.S., Brown, T.A., 2009. Vegetation mediated the impacts of postglacial climatic change on fire regimes in the south-central Brooks Range, Alaska. *Ecol. Monogr.* 79 (2), 201–219.
- Hogg, A., Hua, Q., Blackwell, P., Niu, M., Buck, C., Guilderson, T., Heaton, T., Palmer, J., Reimer, P., Reimer, R., Turney, C., Zimmerman, S., 2013. SHCAL13 southern hemisphere calibration, 0–50,000 years CAL BP. *Radiocarbon* 55 (4), 1889–1903. https://doi.org/10.2458/azu_js_rc.55.16783.
- Hogg, A.G., Heaton, T.J., Hua, Q., Palmer, J.G., Turney, C.S.M., Southon, J., Bayliss, A., Blackwell, P.G., Boswijk, G., Bronk Ramsey, C., Pearson, C., Petchey, F., Reimer, P., Reimer, R., Wacker, L., 2020. SHCal20 southern hemisphere calibration, 0–55,000 Years cal BP. *Radiocarbon* 62 (4), 759–778. <https://doi.org/10.1017/RDC.2020.59>.
- Holz, A., Veblen, T.T., 2012. Wildfire activity in rainforests in western Patagonia linked to the southern annular mode. *Int. J. Wildland Fire* 21, 114–126. <https://doi.org/10.1071/WF10121>.
- Holz, A., Méndez, C., Borrero, L.A., Prieto, A., Torrejón, F., Maldonado, A., 2016. Fires: the main human impact on past environments in Patagonia 24 (2), 72–73. <https://doi.org/10.22498/pages.24.2.72>.
- Holz, A., Paritsis, J., Mundo, I.A., Veblen, T.T., Kitzberger, T., Williamson, G.J., Aráoz, E., Bustos-Schindler, C., González, M.E., Grau, H.R., Quezada, J.M., 2017. Southern Annular Mode drives multicentury wildfire activity in southern South America. *Proc. Natl. Acad. Sci. U.S.A.* 114 (36), 1–6. <https://doi.org/10.1073/pnas.1705168114>.
- Iglesias, V., Whitlock, C., 2014. Fire responses to postglacial climate change and human impact in northern Patagonia (41–43°S). *Proc. Natl. Acad. Sci. USA* 111, E5545–E5554. <https://doi.org/10.1073/pnas.1410443111>.
- Iglesias, V., Whitlock, C., Bianchi, M.M., Villarosa, G., Outes, V., 2011. Holocene climate variability and environmental history at the Patagonian forest/steppe ecotone: Lago Mosquito (42°29'37.89"S, 71°24'14.57"W) and Laguna del Cóndor (42°20'47.22"S, 71°17'07.62"W). *Holocene* 22 (11), 1297–1307. <https://doi.org/10.1177/0959683611427330>.
- Iglesias, V., Whitlock, C., Markgraf, V., Bianchi, M.M., 2014. Postglacial history of the Patagonian forest/steppe ecotone (41–43°S). *Quat. Sci. Rev.* 94, 120–135. <https://doi.org/10.1016/j.quascirev.2014.04.014>.
- Iglesias, V., Haberle, S.G., Holz, A., Whitlock, C., 2018. Holocene dynamics of temperate rainforests in West-central Patagonia. *Front. Ecol. Evol.* 5, 177. <https://doi.org/10.3389/fevo.2017.00177>.
- Jara, I.A., Moreno, P.I., 2014. Climatic and disturbance influences on the temperate rainforests of northwestern Patagonia (40°S) since ~14,500 cal yr BP. *Quat. Sci. Rev.* 90, 217–228. <https://doi.org/10.1016/j.quascirev.2014.01.024>.
- Jara, I.A., Moreno, P.I., Alloway, B.V., Newham, R.M., 2019. A 15,400-year long record of vegetation, fire-regime, and climate changes from the northern Patagonian Andes. *Quat. Sci. Rev.* 226, 106005. <https://doi.org/10.1016/j.quascirev.2019.106005>.
- Kelly, R.F., Higuera, P.F., Barrett, C.M., Hu, F.S., 2011. A signal-to-noise index to quantify the potential for peak detection in sediment-charcoal records. *Quat. Res.* 75, 11–17. <https://doi.org/10.1016/j.yqres.2010.07.011>.
- Lee, D.Y., Petersen, M.R., Lin, W., 2019. The southern annular mode and southern ocean surface westerly winds in E3SM. *Earth Sp. Sci.* 6, 2624–2643. <https://doi.org/10.1029/2019EA000663>.
- Luebert, F., Pliscoff, P., 2017. *Sinopsis bioclimática y vegetal de Chile*. Editorial Universitaria, Chile.
- Lusk, C.H., 1999. Long-lived light-demanding emergent in southern temperate forest: the case of *Weinmannia trichosperma* (Cunoniaceae) in Chile. *Plant Ecol* 104, 111–115. <https://doi.org/10.1023/A:1009764705942>.
- Maldonado, A., de Porras, M.E., Martel-Cea, A., Reyes, O., Nuevo-Delaunay, A., Méndez, C., 2022. Holocene environmental dynamics of the Lago cochrane/pueyrredón valley, central west Patagonia (47°S). *Front. Earth Sci.* 10, 833637. <https://doi.org/10.3389/feart.2022.833637>.
- Markgraf, V., Bradbury, J.P., Schwab, A., Burns, S.J., Stern, C., Ariztegui, D., Gilli, A., Anselmetti, F.S., Stine, S., Maidana, N., 2003. Holocene palaeoclimates of southern Patagonia: limnological and environmental history of Lago Cardiel, Argentina. *Holocene* 13 (4), 581–591.
- Markgraf, V., Whitlock, C., Haberle, S., 2007. Vegetation and fire history during the last 18,000 cal yr B.P. in southern Patagonia: mallín Pollux, coyhaique, province aisen (45°41'30" S, 71°50'30" W, 640 m elevation). *Palaeogeogr. Palaeoclimatol. Palaeoecol.* 254, 492–507. <https://doi.org/10.1016/j.palaeo.2007.07.008>.
- Marshall, G.J., 2003. Trends in the southern annular mode from observations and reanalyses. *J. Clim.* 16, 4134–4143. [10.1175/1520-0442\(2003\)016%3C4134:TITSAM%3E2.0.CO;2](https://doi.org/10.1175/1520-0442(2003)016%3C4134:TITSAM%3E2.0.CO;2).
- Martín, M., 2005. *De la Trapananda al Aysén* (Santiago, Pehuén).
- McCulloch, R.D., Bentley, M.J., Purves, R.S., Hulton, N.R.J., Dugden, D.E., Clapperton, C.M., 2000. Climatic inferences from glacial and palaeoecological evidence at the last glacial termination, southern South America. *J. Quat. Sci.* 15 (4), 409–417. [https://doi.org/10.1002/1099-1417\(200005\)15:4%3C409:AID-JQS539%3E3.0.CO;2%3](https://doi.org/10.1002/1099-1417(200005)15:4%3C409:AID-JQS539%3E3.0.CO;2%3).
- Méndez, C., Reyes, O., 2008. Late Holocene human occupation of Patagonian forests: a case study at Cisnes River basin (44° S, Chile). *Antiquity* 82, 560–570.
- Méndez, C., Reyes, O., Nuevo Delaunay, A., Trejo, V., Barberena, R., Velásquez, H., 2011. Ocupaciones humanas en la margen occidental de Patagonia Central: eventos de poblamiento en Alto Río Cisnes. *Magallania* 39, 223–224.

- Méndez, C., de Porras, M.E., Maldonado, A., Reyes, O., Nuevo-Delaunay, A., García, J.-L., 2016. Human effects in Holocene fire dynamics in central western Patagonia (−44° S, Chile). *Front. Ecol. Evol.* 4, 100. <https://doi.org/10.3389/fevo.2016.00100>.
- Méndez, C., Nuevo-Delaunay, A., Reyes, O., 2023. The exploration of marginal spaces in Central-West Patagonia and the role of discontinuous occupation of forests and highlands. *L'Anthropologie*, 103118. <https://doi.org/10.1016/j.anthro.2023.103118>.
- Montade, V., Combourieu, N., Kissel, C., Siani, G., Michel, E., Haberle, S., 2013. Vegetation and climate changes during the last 22,000 yr from a marine core near Taitao Peninsula, southern Chile. *Palaeogeogr. Palaeoclimatol. Palaeoecol.* 369, 335–348. <https://doi.org/10.1016/j.palaeo.2012.11.001>.
- Montade, V., Peyron, O., Favier, C., Francois, J.P., Haberle, S.G., 2019. A pollen–climate calibration from western Patagonia for palaeoclimatic reconstructions. *J. Quaternary Sci.* 34, 76–86. <https://doi.org/10.1002/jqs.3082>.
- Moreno, P.I., 2000. Climate, fire and vegetation between about 13,000 and 9200 ¹⁴C yr B.P. in the Chilean Lake District. *Quat. Res.* 54, 81–89. <https://doi.org/10.1006/qres.2000.2148>.
- Moreno, P.I., 2004. Millennial-scale climate variability in northwest Patagonia over the last 15,000 yr. *J. Quat. Sci.* 19, 35–47. <https://doi.org/10.1002/jqs.813>.
- Moreno, P.I., 2020. Timing and structure of vegetation, fire, and climate changes on the Pacific slope of northwestern Patagonia since the last glacial termination. *Quat. Sci. Rev.* 238, 106328. <https://doi.org/10.1016/j.quascirev.2020.106328>.
- Moreno, P.I., Francois, J.P., Moy, C.M., Villa-Martínez, R., 2010a. Covariability of the southern westerlies and atmospheric CO₂ during the Holocene. *Geology* 38 (8), 727–730. <https://doi.org/10.1130/G30962.1>.
- Moreno, P.I., Kitzberger, T., Iglesias, V., Holz, A., 2010b. Paleofires in southern South America since the last glacial maximum. *PAGES News* 18, 75–77. <https://doi.org/10.22498/pages.18.2.75>.
- Moreno, P., Vilanova, I., Villa-Martínez, R., Garreaud, R.D., Rojas, M., De Pol-Holz, R., 2014. Southern Annular Mode-like changes in southwestern Patagonia at centennial timescales over the last three millennia. *Nat. Commun.* 5, 4375. <https://doi.org/10.1038/ncomms5375>.
- Moreno, P.I., Vilanova, I., Villa-Martínez, R., Dunbar, R.B., Mucciarone, D.A., Kaplan, M. R., Garreaud, R.D., Rojas, M., Moy, C.M., Pol-Holz, R.D., Lambert, F., 2018. Onset and evolution of southern annular mode-like changes at centennial timescale. *Sci. Rep.* 8, 3458. <https://doi.org/10.1038/s41598-018-21836-6>.
- Moreno, P.I., Simi, E., Villa-Martínez, R.P., Vilanova, I., 2019. Early arboreal colonization, postglacial resilience of deciduous *Nothofagus* forests, and the Southern Westerly Wind influence in central-east Andean Patagonia. *Quat. Sci. Rev.* 218, 61–74. <https://doi.org/10.1016/j.quascirev.2019.06.004>.
- Moreno, P.I., Videla, J., Kaffman, M.J., Henríquez, C.A., Sagredo, E.A., Jara-Arancio, P., Alloway, B.V., 2021. Vegetation, disturbance, and climate history since the onset of ice-free conditions in the Lago Rossetol sector of Chiloé continental (44°S), northwestern Patagonia. *Quat. Sci. Rev.* 260, 106924. <https://doi.org/10.1016/j.quascirev.2021.106924>.
- Moreno, P.I., Méndez, C., Henríquez, C.A., Fercovic, E.I., Videla, J., Reyes, O., Villacís, L. A., Villa-Martínez, R., Alloway, B.V., 2023. Fires and rate of change in the temperate rainforest of northwestern Patagonia since ~18 ka. *Quat. Sci. Rev.* 300, 107899. <https://doi.org/10.1016/j.quascirev.2022.107899>.
- Mundo, I.A., González, C.V., Stoffel, M., Ballesteros-Cánovas, J.A., Villalba, R., 2019. Fire damage to cambium affects localized xylem anatomy and hydraulics: the case of *Nothofagus pumilio* in Patagonia. *Am. J. Bot.* 106 (12), 1536–1544. <https://doi.org/10.1002/ajb2.1395>.
- Nanavati, W.P., Whitlock, C., Iglesias, V., de Porras, M.E., 2019. Postglacial vegetation, fire, and climate history along the eastern Andes, Argentina and Chile (lat. 41–55°S). *Quat. Sci. Rev.* 207, 145–160. <https://doi.org/10.1016/j.quascirev.2019.01.014>.
- Naranjo, J.A., Stern, C.R., 2004. Holocene tephrochronology of the southernmost part (42°30'–45°S) of the Andean southern volcanic zone. *Rev. Geol. Chile* 31 (2), 225–240.
- Otero, L., 2006. La huella del fuego. Historia de los bosques nativos. Poblamiento y cambios en el paisaje del sur de Chile. Pehuén, Chile.
- Paritsis, J., Veblen, T.T., Holz, A., 2015. Positive fire feedbacks contribute to shifts from *Nothofagus pumilio* forests to fire-prone shrublands in Patagonia. *J. Veg. Sci.* 26, 89–101. <https://doi.org/10.1111/jvs.12225>.
- Paruelo, J.M., Beltrán, A., Jobbágy, E., Sala, O.E., Golluscio, R.A., 1998. El clima de la Patagonia: patrones generales y controles sobre los procesos bióticos. *Ecol. Austral* 8, 85–101.
- Pesce, O.H., Moreno, P.I., 2014. Vegetation, fire and climate change in central-east Isla Grande de Chiloé (43°S) since the Last Glacial Maximum, northwestern Patagonia. *Quat. Sci. Rev.* 90, 143–157. <https://doi.org/10.1016/j.quascirev.2014.02.021>.
- Promis, A., Bergh, G., Serra, M.T., Cruz, G., 2013. Descripción de la flora vascular en el sotobosque de un bosque pantanoso y de una pradera antropogénica húmeda de *Juncus procerus* en el valle del río Cisnes, Región de Aysén, Chile. *Gayana. Bot.* 70 (1), 164–169.
- Quade, J., Kaplan, M.R., 2017. Lake-Level stratigraphy and geochronology revisited at Lago (Lake) cardiel, Argentina, and changes in the southern hemispheric westerlies over the last 25 ka. *Quat. Sci. Rev.* 177, 173–188. <https://doi.org/10.1016/j.quascirev.2017.10.006>.
- Quintanilla, V., 2008. Perturbaciones a la vegetación nativa por grandes fuegos de 50 años atrás, en bosques nordpatagónicos. Caso de estudio en Chile Meridional. *An. de Geog.* 28 (1), 85–104.
- R Development Core Team, 2013. R: A Language and Environment for Statistical Computing. R Foundation for Statistical Computing, Vienna, Austria. ISBN 3-900051-07-0, URL. <http://www.r-project.org>.
- Retamales, H., 2021. *Mirtáceas en la flora silvestre de Chile: historia natural y situación actual*. Chile. Primera edición 228.
- Sistema de Información Territorial (SIT), 2020. CONAF. <https://sit.conaf.cl/>. (Accessed 10 June 2023).
- Szeicz, J.M., Zeeb, B.A., Bennett, K.D., Smol, J.P., 1998. High-resolution paleoecological analysis of recent disturbance in a southern Chilean *Nothofagus* forest. *J. Paleolimnol.* 20, 235–252. <https://doi.org/10.1023/A:1007950905200>.
- Ter Braak, C.J.F., Smilauer, P., 2012. CANOCO Reference Manual and CanoDraw for Windows User's Guide: Software for Canonical Community Ordination (Version 5.0). Microcomputer Power, Ithaca, NY, USA. Available at: <http://www.Canoco.com/>.
- Thorndyck, V.R., Bendle, J.M., Benito, G., Davies, B.J., Sancho, C., Palmer, A.P., Fabel, D., Medialdea, A., Martin, J.R.V., 2019. Glacial lake evolution and Atlantic-Pacific drainage reversals during deglaciation of the Patagonian Ice Sheet. *Quat. Sci. Rev.* 203, 102–127. <https://doi.org/10.1016/j.quascirev.2018.10.036>.
- Tiribelli, F., Kitzberger, T., Morales, J.M., 2018. Changes in vegetation structure and fuel characteristics along post-fire succession promote alternative stable states and positive fire–vegetation feedbacks. *J. Veg. Sci.* 29 (2), 147–156. <https://doi.org/10.1111/jvs.12620>.
- Viale, M., Bianchi, E., Cara, L., Ruiz, L.E., Villalba, R., Pitte, P., Masiokas, M., Rivera, J., Zalazar, L., 2019. Contrasting climates at both sides of the Andes in Argentina and Chile. *Front. Environ. Sci.* 7, 69. <https://doi.org/10.3389/fevs.2019.00069>.
- Vilanova, I., Moreno, P.I., Miranda, C.G., Villa-Martínez, R.P., 2019. The last glacial termination in the Coyhaique sector of Central Patagonia. *Quat. Sci. Rev.* 224, 105976. <https://doi.org/10.1016/j.quascirev.2019.105976>.
- Villa-Martínez, R., Moreno, P.I., 2007. Pollen evidence for variations in the southern margin of the westerly winds in SW Patagonia over the last 12,600 years. *Quat. Sci. Rev.* 68, 400–409. <https://doi.org/10.1016/j.yqres.2007.07.003>.
- Villa-Martínez, R., Moreno, P.I., 2021. Development and resilience of deciduous *Nothofagus* forests since the last glacial termination and deglaciation of the central Patagonian Andes. *Palaeogeogr. Palaeoclimatol. Palaeoecol.* 574, 110459. <https://doi.org/10.1016/j.palaeo.2021.110459>.
- Villa-Martínez, R., Moreno, P.I., Valenzuela, M.A., 2012. Deglacial and postglacial vegetation changes on the eastern slopes of the central Patagonian Andes (47°S). *Quat. Sci. Rev.* 32, 86–99. <https://doi.org/10.1016/j.quascirev.2011.11.008>.
- Weller, D.J., de Porras, M.E., Maldonado, A., Méndez, C., Stern, C.R., 2017. Holocene tephrochronology of the lower Río Cisnes valley, southern Chile. *Andean Geol.* 44 (3), 229–248. <https://doi.org/10.5027/andgeoV44n3-a01>.
- Whitlock, C., Larsen, C., 2001. Charcoal as a proxy fire. In: Smol, J.P., Birks, H.J.B., Last, W.M. (Eds.), *Tracking Environmental Change Using Lake Sediments: Terrestrial, Algal, and Siliceous Indicators*. Kluwer Academic Publishers, Dordrecht, Netherlands, pp. 75–97.
- Whitlock, C., Bianchi, M.M., Bartlein, P.J., Markgraf, V., Marlon, J., Walsh, M., McCoy, N., 2006. Postglacial vegetation, climate, and fire history along the east side of the Andes (lat 41–42.5°S), Argentina. *Quat. Res.* 66, 187–201. <https://doi.org/10.1016/j.yqres.2006.04.004>.